Inducible Astrocytic Glucose Transporter-3 Contributes to the Enhanced Storage of Intracellular Glycogen during Reperfusion after Ischemia

SADAHIRO IWABUCHI, KOICHI KAWAHARA*

Laboratory of Cellular Cybernetics, Graduate School of Information Science and Technology, Hokkaido University, Sapporo, Japan

Address correspondence to:

Koichi Kawahara, PhD

Professor of the Laboratory of Cellular Cybernetics, Graduate School of Information Science and Technology, Hokkaido University, Sapporo 060-0814, Japan

PHONE&FAX: +81-11-706-7591

E-mail: kawahara@ist.hokudai.ac.jp

Abstract

Glucose is a necessary source of energy to sustain cell activities and homeostasis in the brain, and enhanced glucose transporter (GLUT) activities are protective of cells during energy depletion including brain ischemia. Here we investigated whether and if so how the astrocytic expression of GLUTs crucial for the uptake of glucose changes in ischemic conditions. Under physiological conditions, cultured astrocytes primarily expressed GLUT1, and GLUT3 was only detected at extremely low levels. However, exposure to ischemic stress increased the expression of not only GLUT1 but also GLUT3. During ischemia, cultured astrocytes significantly increased production of the transcription factor nuclear factor-κB (NF-κB), leading to an increase in GLUT3 expression. Moreover, astrocytic GLUT3 was responsible for the enhanced storage of intracellular glucose during reperfusion, resulting in increased resistance to lethal ischemic stress. These results suggested that astrocytes promptly increase GLUT3 production in situations such as ischemia, and much glucose is quickly taken up, possibly contributing to the protection of astrocytes from ischemic damage.

Key words

Astrocytes, GLUT3, GLUT1, Ischemic stress, Glycogen

Abbreviations

GLUT: glucose transporter, HE: Hoechst 33342, IKK: inhibitor of κB kinase, NF-κB: nuclear factor-κB, OGD: oxygen glucose deprivation, PC: preconditioning

1. Introduction

Energy-independent glucose transporters (GLUTs), which contain 12 membrane-spanning domains and span the plasma membrane, mediate the entry or exit of glucose. Thirteen facilitative GLUTs have been identified (Wood and Trayhurn, 2003), the predominant cerebral GLUTs being GLUT1 and GLUT3. GLUT2, GLUT4, GLUT5, and GLUT7 have also been detected at low levels in the brain (Vannucci et al., 1997). Under physiological conditions, GLUT1 is mainly expressed at plasma membranes in astrocytes, and GLUT3 is expressed not in astrocytes but in neurons (Maher et al., 1994). The parameters of neuronal GLUT3 activities such as kinetics or catalytic center activity (CCA) determined by conducting assays using a non-metabolizable glucose analog show that the entry-mode velocity (CCA value) of GLUT1 and GLUT3 is 123 and 853 (s^{-1}), respectively, revealing that GLUT3 transports extracellular glucose about 7 times faster than GLUT1 (Maher et al., 1996). GLUT3 only takes up extracellular glucose: it does not release intracellular glucose to the extracellular space even if the intracellular glucose concentration is higher than the extracellular concentration. Therefore, it seems reasonable that neurons strongly express GLUT3 under physiological conditions, because glucose is a necessary source of energy to sustain neuronal activities.

A number of studies have demonstrated that enhanced glucose transporter activities are protective of cells during energy depletion (Vannucci et al., 1997; Vannucci et al., 1998; Yu et al., 2008). Hypoxic insults increase GLUT1 mRNA and protein levels in astrocytic cultures,

and sublethal hypoxic insults, i.e., hypoxic preconditioning, up-regulates the expression of neuronal GLUT1 and GLUT3 mRNA as well as astrocytic GLUT1 mRNA, leading to the development of hypoxic tolerance (Vannucci et al., 1998). However, it is still unknown whether GLUT3 is actually expressed in astrocytes under pathological conditions or not.

Astrocytes are reactive in response to ischemic stress: they become hypertrophic and glial fibrillary acidic protein (GFAP) expression is increased. Such reactive astrocytes possibly contribute to the induction of neuronal migration or the growth of axons during development (Rakic, 1971), and have a protective role in the central nervous system under pathological conditions (Li et al., 2008). Our previous study showed that the exposure of cultured astrocytes to sublethal ischemia, preconditioning (PC), results in a marked increase in GFAP, and such astrocytes have increased resistance to subsequent lethal ischemic stress (Iwabuchi and Kawahara, 2009). In contrast, controversial results suggest that reactive astrocytes interfere with axonal regeneration in the injured spinal cord (Brown and Mc, 1947). In addition, it is unclear whether changes in the expression and activity of GLUT3 are involved in the PC-induced ischemic tolerance in astrocytes.

In this study, we found that in cultured astrocytes, the expression of GLUT3 increased under ischemic conditions, and the increase was responsible for an increase in the amount of glycogen deposited during reperfusion, contributing to the development of resistance to subsequent lethal ischemic stress.

2. Materials and methods

2.1 Cell culture

The animal experiments were carried out in accordance with *The Guide for the care and use of laboratory animals*, Hokkaido University School of Medicine. The methods used to obtain primary astrocytic cultures were described previously in detail (Iwabuchi and Kawahara, 2011; Kawahara et al., 2002). In brief, the cortical hemispheres of postnatal 2 to 3-day-old rats, were isolated and digested at 37 °C for 30 min with a 0.01% papain-cysteine solution. Primary astrocytes were plated onto polyethyleneimine-coated glass coverslips/plastic dishes at 20,000 cells/cm^2. Cells were maintained with a culture medium (CM) (80% Dulbecco's modified Eagle's medium (Gibco, Grand Island, USA) supplemented with 10% Ham's F-12 nutrient mixture and 10% fetal bovine serum) with 1% penicillin/streptmycin at 37 °C in a 5% CO_2 incubator. Cultured astrocytes were fed a cooled CM twice a week. The experiments were performed with cultures maintained for 14-21 days.

2.2 Oxygen-glucose deprivation (OGD)

Cultures were washed two times with a glucose-free balanced salt solution (BSS: supplemented with 142 mM NaCl, 0.8 mM $MgSO_4$, 5.4 mM KCl, 1.0 mM NaH_2PO_4, 4 mM $NaHCO_3$, 1.8 mM $CaCl_2$ and 0.01 mM glycine),

and placed in an anaerobic chamber containing the de-oxygenation reagent (an O_2 concentration of < 1% during 1 h; Mitsubishi Gas Chemical, Tokyo, Japan) at 37 °C. To terminate the OGD treatment, the BSS buffer in each culture was removed carefully and cultures were incubated with fresh or warm CM at 37 °C in a 5% CO_2 incubator for 1 h or 1 day (reperfusion period). The intracellular glycogen concentration in astrocytes was assessed with assay an EnzyChrom™ Glycogen Assay Kit (BioAssay Systems, Hayward, USA) according to the manufacturer's instructions. The reagent combines the enzymatic break down of glycogen, detecting glucose. The luminescence intensity of each well at 570 nm was determined using a microplate reader (Infinite®200; Tecan Austria GmbH, Salzburg, Austria).

2.3 Real-time Reverse transcription polymerase chain reaction (RT-PCR)

Total RNA in each astrocytic culture was obtained using the RNA extraction reagent: ISOGEN (Molecular Research Center, Cincinnati, USA), and then complementary DNA (cDNA) product was synthesized by PrimeScript® Reverse Transcriptase (Takara Bio, Shiga, Japan), oligo (dT)12-18 primer and deoxy nucleotide triphosphate (dNTP) mixture (Promega, Madison, USA), according to the manufacturer's instructions. The PCR primer pairs and probes for GLUT1, GLUT3, an IκB-nuclear factor-κB (NF-κB), and α-actin were designed as follows; GLUT1 [NCBI reference sequence: NM_138827.1; (sense)

5’-AGTATCGTGGCCATCTTTGG-3’, (antisense) 5’-GCCACAATGAACCATGGAA-3’, (probe) 5’-GGCCCTGG-3’], GLUT3[NM_017102.2; (sense) 5’-TCTCTGGGATCAATGCTGTG-3’, (antisense) 5’-CCAATCGTGGCATAGATGG-3’, (probe) 5’-GTGTCCAG-3’], NF-κB[XM_342346.4; (sense) 5’-ATCGCTCA -GGCCCACTTG-3’, (antisense) 5’-TGTCATTATCTCGGAGCTCATCT-3’, (probe) 5’-CTCCTCCA-3’], α-actin [NM_017008.3; (sense) 5’-AATGTATCCGTTGTGGATCTGA-3’, (antisense) 5’-GCTTCACCACCTTCTTGATGT-3’, (probe) 5’-CCTGGAGA-3’]. AmpliTaq Gold® PCR Master Mix (Life Technologies, California, USA) was added to each sample, and then cDNA was amplified with a thermal cycler. α-actin was used as the housekeeping gene to standardize GLUT1, GLUT3, and NF-κB mRNA levels.

2.4 Western blot analysis

Western blotting was performed as described previously in detail (Iwabuchi and Kawahara, 2009, 2011). In brief, cell lysate in a sodium dodecyl sulfate (SDS) sample buffer was electrophoresed on SDS Tris-HCl gels (DRC, Tokyo, Japan), and transferred to PVDF membranes (Amersham, Arlington Heights, USA). The blots were blocked, and specific proteins were detected by using as primary antibodies, anti-rabbit IgG anti-GLUT1 (IBL, Gunma, Japan; 1:1000), GLUT3 (Abcam, Cambridge, UK; 1:1000) and anti-mouse IgG anti-β-actin (Sigma-Aldrich, St. Louis, USA; 1:10000). The signals

were visualized using an enhanced chemiluminescence system (NEN Life Science Products, Boston, USA). Quantification of the immunoreactive bands was done with Scion Image for Windows (Scion Corporation, Frederick, USA). Quantitative evaluation of the expression of each protein was performed as described (Iwabuchi and Kawahara, 2009). We measured the density of these bands, and calculated the rate for total β-actin in control or OGD groups. We took the values in control groups to be 100%, and then calculated the rate in OGD groups.

2.5 Immunocytochemistry

Cells were fixed with 4% paraformaldehyde and washed with phosphate-buffered saline (PBS). To detect the positive reactions in the cellular membranes, a detergent such as Triton-X was not used. Fixed-cells were then treated with 1% normal goat serum for 30 min. Immunofluorescent labeling was done with antibodies directed against GLUT1 (IBL; 1:200), GLUT3 (Abcam; 1:200). Negative controls without each primary antibody were also performed. Each primary antibody was visualized with Alexa Fluor 488-conjugated anti-rabbit antibodies (Invitrogen, Karlsruhe, Germany; 1:200). The fluorescent DNA-binding dye, Hoechst 33342 (HE), was used to detect nuclei. The immunoreactivity was observed with a confocal laser scanning microscope (FV300; Olympus, Tokyo, Japan). The image analysis was identical for each culture. In single astrocytic cultures, more than 94% cells were astrocytes as described

previously (Iwabuchi and Kawahara, 2009; Kawahara et al., 2002).

2.6 RNA interference

RNA interference for newly synthesized GLUT3 mRNA was performed with the use of small interfering RNA, mouse GLUT3 (Santa Cruz Biotechnology, California, USA). When astrocytes were about 80% confluent, the CM was replaced with a penicillin/streptomycin-free CM and cultured for 1 day. siRNA Transfection Reagent mixture [about 98% siRNA Transfection Medium (Santa Cruz Biotechnology) with 0.6-0.8% GLUT3 siRNA or Control siRNA (Santa Cruz Biotechnology) supplemented with 0.8% siRNA Transfection Reagent (Santa Cruz Biotechnology)] was added to the cultures and incubated for 8 hours. Then CM containing 2 times the volume of fetal bovine serum was added and cultures were incubated for 1 day. Finally, the CM was aspirated and replaced with fresh CM for 1day.

2.7 Cell survival assay

Cell viability was assessed by the 3-(4,5-Dimethyl 2-thiazol)-2,5-diphenyl-*2H*-tetrazolium bromide (MTT) assay (DOJINDO Laboratories, Kumamoto, Japan), which is based on the reduction of the yellow MTT tetrazolium salt by mitochondrial dehydrogenases to form a blue MTT formazan. A MTT dissolved-solution was added to each well and

incubated for 3 h, and the medium was removed completely and a 40 mM HCl-isopropanol lysis buffer was added. The optical density of each well at 560 nm was determined using a microplate reader (Infinite®200; Tecan Austria GmbH).

2.8 Data analysis

The data are expressed as the mean ± standard error of the mean (S.E.M.). Comparisons were performed using the ANOVA followed by a paired Student's *t*-test or Student's *t*-test alone. Differences at $p < 0.05$ were considered significant.

3. Results

3.1 OGD-induced increase in astrocytic GLUT3 expression

The Real-time PCR analysis showed that both GLUT1 and GLUT3 mRNA levels increased significantly during the simulated ischemia (oxygen and glucose deprivation: OGD) (Fig.1A&B). The expression of GLUT1 mRNA increased with the duration of OGD. GLUT1 mRNA was readily detected in cultured astrocytes in the control group; however, astrocytic GLUT3 mRNA was rarely detected (0.00007 ± 0.0001, mean ± S.E.M.). In contrast to GLUT1 mRNA, the relative GLUT3 mRNA levels were significantly higher at 1 h of OGD (0.002 ± 0.09, mean ± S.E.M.) than 2 h of OGD (0.007 ± 0.002).

The Western blot analysis revealed that the expression of the 50kDa form of GLUT1 at 2 h of OGD was 147.3 ± 17.3% (mean ± S.E.M.), and a significant increase in GLUT1 expression was observed as compared to the control groups (100.0 ± 6.4%) (Fig.1C, white bars). The expression of the 54kDa form of GLUT3 in OGD groups was also significantly increased, by 2.3-fold (Fig.1C, black bars). To further confirm the OGD-induced increase in GLUTs expression in astrocytes, an immunofluorescent analysis was performed. Two hours of OGD treatment enhanced both GLUT1 and GLUT3-positive reactions (green) as compared to the control (Fig.1D).

3.2 The transcription factor NF-κB regulates the increase in GLUT3

expression

It has been reported that the activation of an IκB-nuclear factor-κB (NF-κB) pathway causes the upregulation of GLUT3 mRNA expression in mouse embryonic fibroblasts (Kawauchi et al., 2008). In addition, endothelin-1's induction of GLUT1 transcription is mediated by NF-κB in cultured adipocytes (Kao and Fong, 2008). Therefore, we speculated that NF-κB might regulate the synthesis of astrocytic GLUTs during OGD. An inhibitor of IKKα and IKKβ, wedelolactone (50 μM), was added to the glucose-free BSS and the cultures were exposed to OGD. As expected, the increase in both GLUT1 (Fig.2A) and GLUT3 (Fig.2B) mRNA levels was significantly attenuated in the OGD groups treated with wedelolactone.

Western blotting and immunofluorescence analyses revealed that wedelolactone significantly suppressed astrocytic GLUTs expression in the OGD groups (Fig. 2C&D). Notably, the increase in GLUT3 expression was strongly attenuated by wedelolactone treatment [OGD2h with or without wedelolactone: 32.4 ± 5.5 or 100.0 ± 1.4% (mean ± S.E.M.)]. Fig. 2E shows that OGD significantly increased NF-κB mRNA levels as compared to the control, and the increase was dependent on the duration of OGD. Wedelolactone itself inhibited the synthesis of NF-κB mRNA (Fig. 2E). When an inhibitor of protein synthesis, cycloheximide (50 μM), was added to the BSS and exposed to OGD, both mRNA and protein levels of GLUTs were significantly decreased (Fig. 2A-2D).

3.3 Functional significance of GLUT3 expression in astrocytes

Treatment of astrocytes with GLUT3 siRNA resulted in a significant decrease of GLUT3 expression as revealed by both Western blot and immunocytochemical analyses (Fig. 3A&B). The intracellular glycogen levels at 1 h reperfusion after OGD were significantly lower than control values (Fig. 3C). However, the levels at 1 day of reperfusion after OGD were significantly increased as compared to the control. In contrast, the increase in intracellular glycogen was suppressed in the GLUT3 siRNA-treated groups. We then investigated whether the increase in intracellular glycogen deposition was involved in the protection of astrocytes from subsequent lethal ischemic stress. After 1 day of reperfusion following 2 h of OGD, the cultures were again exposed to OGD stress. As shown in Fig. 3D, preconditioned (PC) astrocytes exhibited resistance to subsequent lethal OGD. Eight hours of lethal OGD significantly increased astrocytic cell damage as compared to that in the PC astrocytes. The PC-induced increased resistance was significantly attenuated in cells treated with GLUT3 siRNA. In addition, GLUT3 siRNA treatment did not affect the expression of GLUT1 mRNA and protein (Fig. 4), further supporting our inference that the PC-induced increase in GLUT3 was crucial to the increased glucose uptake, leading to the development of resistance to lethal ischemia.

4. Discussion

4.1 Ischemic stress induces GLUT3 expression via NF-κB's signaling pathways

Our findings demonstrate that astrocytes enhance not only GLUT1 but also GLUT3 protein expression under ischemic conditions. NF-κB's signaling pathways increase both astrocytic GLUT3 mRNA and protein levels in astrocyte-enriched cultures. GLUT3 only takes up extracellular glucose, it does not release intracellular glucose even if its concentration is higher than that of extracellular glucose ($[GLU]_e$). Therefore, it seems reasonable that neurons strongly express GLUT3 under physiological conditions, because glucose is a necessary source of energy to sustain neuronal activities. What if neuronal GLUTs expression occurs under pathological conditions? Immediately after anoxic or ischemic insults, stressed neurons increase their own GLUT3 gene expression, and additionally, enhanced GLUT1 mRNA expression is also observed (Vannucci et al., 1998; Yu et al., 2008). These phenomena imply that glucose transport is critical for neurons to survive under pathological conditions. In contrast, glucose is mainly taken up through GLUT1 in astrocytes. When the extracellular concentration of glucose is low, astrocytes also increase their GLUT1 mRNA both *in vivo* and *in vitro* (Vannucci et al., 1998; Yu et al., 2008), suggesting this inherent response to be pivotal for astrocytes to avoid acute or delayed cell death under anoxic or ischemic conditions. In addition, GLUT3 mRNA is not

detectable in astrocytes after hypoxic stress (Yu et al., 2008). However, using established techniques for anoxic or ischemic insults, the loading period for the anoxic gas mixture is generally determined by the neuronal response to the stress, i.e., the stress is sublethal or lethal to neurons, but these conditions may be less than sublethal to astrocytes.

Contrary to in previous studies (Vannucci et al., 1998; Yu et al., 2008), GLUT3 protein was detected at low levels in control astrocytes (Fig.1). The immunofluorescent analysis also showed the translocation of GLUT3 from the cytoplasm to plasma membrane after OGD (Fig. 1D: lower figure). Though primary neurons were used as GLUT3-positive controls, we initially suspected that the antibody used was not specific to the GLUT3 protein. Therefore, a Western blot analysis of GLUT3 expression with another anti-GLUT3 antibody (IBL, Gunma, Japan) was performed. Nevertheless, GLUT3 expression was similarly observed in the control groups although the expression was low, and 2 h of OGD increased the level about 1.3 fold (data not shown). Additional evidence for the enhancement of astrocytic GLUT3 expression comes from another report. Cidad P et al. showed that the endotoxin lipopolysaccharide (LPS) increased intracellular nitrite (NO_2^-) concentrations, and GLUT3 expression in rat astrocytic cultures was enhanced, leading to an increase in glucose uptake activity (Cidad et al., 2001). These results seem meaningful, but the astrocytic cytotoxicity of LPS (1 μg/mL) and signal transduction regulating the GLUT3 gene are unknown. The transcription factor Sp1 or NF-κB seems to play an important role in the regulation of the GLUT1 gene.

Vasoconstrictor Endothelin-1 (ET-1) induced GLUT1 gene expression via PKCε or MAPK signaling pathways through Sp1 and NF-κB in 3T3-L1 adipocytes (Kao and Fong, 2008). In addition, some oncogenes down-regulate p53 activity, leading to the activation of IKKα or IKKβ and to NF-κB downstream, resulting in the up-regulation of GLUT3 gene expression (Kawauchi et al., 2008). In the present study, NF-κB mRNA levels increased markedly during OGD, and wedelolactone (50 μM) treatment induced significant decreases in GLUTs mRNA and protein, and the protein synthesis inhibitor cycloheximide (100 μM) also suppressed GLUTs expression (Fig. 2). These results suggest that NF-κB's signaling pathways contribute to the increase in not only mRNA but also protein levels of GLUT3 in astrocytic cultures. Further research is needed to investigate how levels of NF-κB mRNA induce GLUT3 expression since the transcription factor regulates both GLUT1 and GLUT3.

4.2 Functional significance of the ischemia-induced increase in GLUT3 expression

Astrocytes could transport extracellular glucose through enhanced GLUT activities when they were recovered from the OGD. The glucose was quickly consumed to recover or sustain the homeostasis of cells; therefore, intracellular glycogen levels might be lower at 1 h of reperfusion (Fig. 3C). The amount of glycogen was significantly increased at 1 day of reperfusion as compared to the control. The results imply that inducible GLUT3 might

support GLUT1 activities, leading to the enhancement of glucose uptake into the astrocytes during reperfusion after ischemia. When astrocytes were treated with siRNA for GLUT3 mRNA, the ischemia-induced increase in intracellular glycogen was significantly attenuated: the intracellular glycogen levels in siGLUT3-treated astrocytes were not significantly different to those in cells of the control groups (Fig. 3C). These results are unexpected since GLUT1 mRNA levels were more increased after OGD as compared to GLUT3 mRNA levels (Fig. 1), and the primary GLUT in astrocytes is GLUT1; therefore, we speculated that the increase in glycogen was mainly regulated by enhanced GLUT1 expression, and inducible GLUT3 expression might make a slight contribution. To understand the precise role of GLUTs in glycogen deposition under pathological conditions, additional experiments using siRNA for GLUT1 mRNA are needed.

The question then arises as to why astrocytes need to accumulate much more intracellular glycogen under pathological conditions. Our previous report indicates many strongly GFAP-positive astrocytes at 1 day of reperfusion after 2 h of OGD, and that such reactive astrocytes are more resistant to subsequent lethal OGD (Iwabuchi and Kawahara, 2009). Ischemic resistance to 8 h of lethal OGD was also seen in astrocytes treated with scrambled RNA for GLUT3 mRNA (siCont), but the tolerance was significantly attenuated in cells treated with siGLUT3 (Fig. 3D). These findings suggest extracellular glucose to be transported through enhanced-GLUT3 activity early in the reperfusion after OGD, leading to

the acceleration of glycogen synthesis and/or storage during 1 day of reperfusion, and much glycogen to be available to resist against subsequent lethal OGD. Further studies are needed to investigate whether ischemic stress enhances astrocytic GLUT3 expression and increases the intracellular glycogen store in an *in vivo* ischemic model. Astrocytes with ischemic tolerance would survive under severe ischemic conditions, and probably contribute to the protection of neurons from ischemic damage in the brain.

Acknowledgements

The analysis of immunoreactivity was carried out with a confocal laser scanning microscope; FV300 at the OPEN FACILITY, Hokkaido University Sousei Hall. This research was supported by a Research Fellowship of the Japan Society for the Promotion of Science to S. I. It was also partly supported by grants-in-aid for scientific research from the Ministry of Education, Science, and Culture of Japan (21650103 & 22300148) to KK.

References

Brown, J.O., Mc, C.G., 1947. Abortive regeneration of the transected spinal cord. The Journal of comparative neurology 87, 131-137.

Cidad, P., Garcia-Nogales, P., et al., 2001. Expression of glucose transporter GLUT3 by endotoxin in cultured rat astrocytes: the role of nitric oxide. Journal of neurochemistry 79, 17-24.

Iwabuchi, S., Kawahara, K., 2009. Possible involvement of extracellular ATP-P2Y purinoceptor signaling in ischemia-induced tolerance of astrocytes in culture. Neurochemical research 34, 1542-1554.

Iwabuchi, S., Kawahara, K., 2011. Functional significance of the negative-feedback regulation of ATP release via pannexin-1 hemichannels under ischemic stress in astrocytes. Neurochemistry international 58, 376-384.

Kao, Y.S., Fong, J.C., 2008. Endothelin-1 induces glut1 transcription through enhanced interaction between Sp1 and NF-kappaB transcription factors. Cellular signalling 20, 771-778.

Kawahara, K., Hosoya, R., et al., 2002. Selective blockade of astrocytic glutamate transporter GLT-1 with dihydrokainate prevents neuronal death during ouabain treatment of astrocyte/neuron cocultures. Glia 40, 337-349.

Kawauchi, K., Araki, K., et al., 2008. p53 regulates glucose metabolism through an IKK-NF-kappaB pathway and inhibits cell transformation. Nature cell biology 10, 611-618.

Li, L., Lundkvist, A., et al., 2008. Protective role of reactive astrocytes in brain ischemia. J Cereb Blood Flow Metab 28, 468-481.

Maher, F., Davies-Hill, T.M., et al., 1996. Substrate specificity and kinetic parameters of GLUT3 in rat cerebellar granule neurons. The Biochemical journal 315 (Pt 3), 827-831.

Maher, F., Vannucci, S.J., et al., 1994. Glucose transporter proteins in brain. Faseb J 8, 1003-1011.

Rakic, P., 1971. Neuron-glia relationship during granule cell migration in developing cerebellar cortex. A Golgi and electronmicroscopic study in Macacus Rhesus. The Journal of comparative neurology 141, 283-312.

Vannucci, S.J., Maher, F., et al., 1997. Glucose transporter proteins in brain: delivery of glucose to neurons and glia. Glia 21, 2-21.

Vannucci, S.J., Reinhart, R., et al., 1998. Alterations in GLUT1 and GLUT3 glucose transporter gene expression following unilateral hypoxia-ischemia in the immature rat brain. Brain Res Dev Brain Res 107, 255-264.

Wood, I.S., Trayhurn, P., 2003. Glucose transporters (GLUT and SGLT): expanded families of sugar transport proteins. The British journal of nutrition 89, 3-9.

Yu, S., Zhao, T., et al., 2008. Hypoxic preconditioning up-regulates glucose transport activity and glucose transporter (GLUT1 and GLUT3) gene expression after acute anoxic exposure in the cultured rat hippocampal neurons and astrocytes. Brain research 1211, 22-29.

Figure Legends

Fig.1 OGD increases GLUT expression. **A&B:** The level of GLUT1 (A) or GLUT3 (B) mRNA relative to α-actin mRNA was determined by real-time PCR. Data are expressed as the mean ± S.E.M. (n = 6, different cultures). $^{**}p < 0.01$ vs GLUT expression in control groups (cont). **C:** Western blot analysis of GLUTs and β-actin. A quantitative evaluation of GLUTs expression relative to β-actin was performed, with level in control groups taken to be 100%. Data are expressed as the mean ± S.E.M. (n = 10, different cultures). $^{**}p < 0.01$ vs GLUT1 expression (white bars), and $^{\#\#}p < 0.01$ vs GLUT3 expression (black bars) in control groups. **D:** Representative immunofluorescent images. GLUT1 (upper images) or GLUT3 (lower images)-positive astrocytes (green) and cell nuclei stained with Hoechst 33342 (blue) in control groups or OGD groups are shown. Scale bars indicate 100 μm.

Fig.2 OGD-induced GLUTs expression is regulated through NF-κB's signaling pathways. During OGD, wedelolactone (50 μM) or cycloheximide (100 μM) was added to the cultures and then a real-time PCR or Western blot analysis of GLUTs was performed. **A&B:** Relative expression of GLUT1 (A) or GLUT3 (B) mRNA. Data are expressed as the mean ± S.E.M. (n = 4, different cultures). $^{**}p < 0.01$ vs GLUTs expression at 1 h of OGD (OGD1h), and $^{\#\#}p < 0.01$ vs GLUTs expression at 2 h of OGD (OGD2h). wedelo: wedelolactone treatment groups, cyclo:

cycloheximide treatment groups. **C:** Upper images are representative images of the control, 2 h of OGD with or without each inhibitor. Data are expressed as the mean ± S.E.M. (n = 4, different cultures). The rate of GLUTs/β-actin expression at 2 h of OGD was taken to be 100%, and used to calculate the rate of GLUTs/β-actin expression at 2 h of OGD with each inhibitor. These inhibitors significantly suppressed the increase in GLUT1 (white bars) and GLUT3 (black bars). $^{*}p < 0.05$, $^{**}p < 0.01$ or $^{\#}p < 0.05$, $^{\#\#}p < 0.01$ vs 2 h of OGD. **D:** Representative immunofluorescent images. GLUTs-positive astrocytes (green) and their nuclei (blue) at 2 h of OGD with or without the inhibitor. Scale bars indicate 200 μm. **E:** Relative expression of NK-κB mRNA. Data are expressed as the mean ± S.E.M. (n = 6, different cultures). $^{**}p < 0.01$ vs control groups, and $^{++}p < 0.01$ vs each OGD groups.

Fig.3 Sublethal ischemia-induced increase of GLUT3 expression contributed to the development of tolerance against subsequent lethal ischemic stress. **A:** GLUT3 expression was significantly down-regulated in GLUT3 siRNA-treated astrocytes. Astrocytes were treated with scrambled (siCont) or GLUT3 siRNA (siGLUT3), and then exposed to sOGD. Representative results are shown. Lane 1; sOGD, lane 2; Control siRNA-treated astrocytes, lane 3; GLUT3 siRNA-treated astrocytes. Data are expressed as the mean ± S.E. (n = 8, different cultures). $^{*}p < 0.05$ vs sOGD groups. **B:** Representative GLUT3-immunofluorescent images. GLUT3-positive astrocytes (green) and their nuclei (HE, blue) in sOGD

groups or GLUT3 siRNA-treated groups. Scale bar indicates 100 μm. **C:** Levels of glycogen at 1 h or 1 day of reperfusion after 2 h of OGD measured with a glycogen-assay kit. The data indicate optical density values at 570 nm, and are expressed as the mean ± S.E. (n = 6, different cultures). The levels were low at 1 h of reperfusion, but were increased as compared to the control at 1 day of reperfusion. $^{**}p < 0.01$ vs control (Cont) groups, $^{\#\#}p < 0.01$ vs 1 day of reperfusion. **D:** The increase in GLUT3 expression was associated with resistance to lethal OGD stress. Cell viability was determined by MTT-assay. The diagram shows the experimental protocol. The viability levels in PC (2 h of OGD)-treated groups were taken to be 100%. Data are expressed as the mean ± S.E. (n = 7, different cultures). $^{**}p < 0.01$ vs lethal OGD without PC, $^{\#\#}p < 0.01$ vs PC treatment.

Fig.4 Expression of GLUT1 was not affected by GLUT3 siRNA treatment. **A:** Relative expression for α-actin of GLUT1 mRNA was performed by real-time PCR analysis. Data are expressed as the mean ± S.E.M. (n = 4, different cultures). cont: control, siGLUT3: GLUT3 siRNA-treated groups. **B:** Western blot analysis of GLUT1. A quantitative evaluation of GLUTs expression for β-actin was performed, and each level in control groups was taken to be 100%. Upper images are representative blotting data of GLUT1 and β-actin. Data are expressed as the mean ± S.E.M. (n = 3, different cultures). **C:** Representative GLUT1-immunofluorescent images. GLUT1-positive astrocytes (green) and their nuclei (HE, blue) in the

control (cont) or GLUT3 siRNA-treated groups (siGLUT3). Scale bar indicates 100 μm.

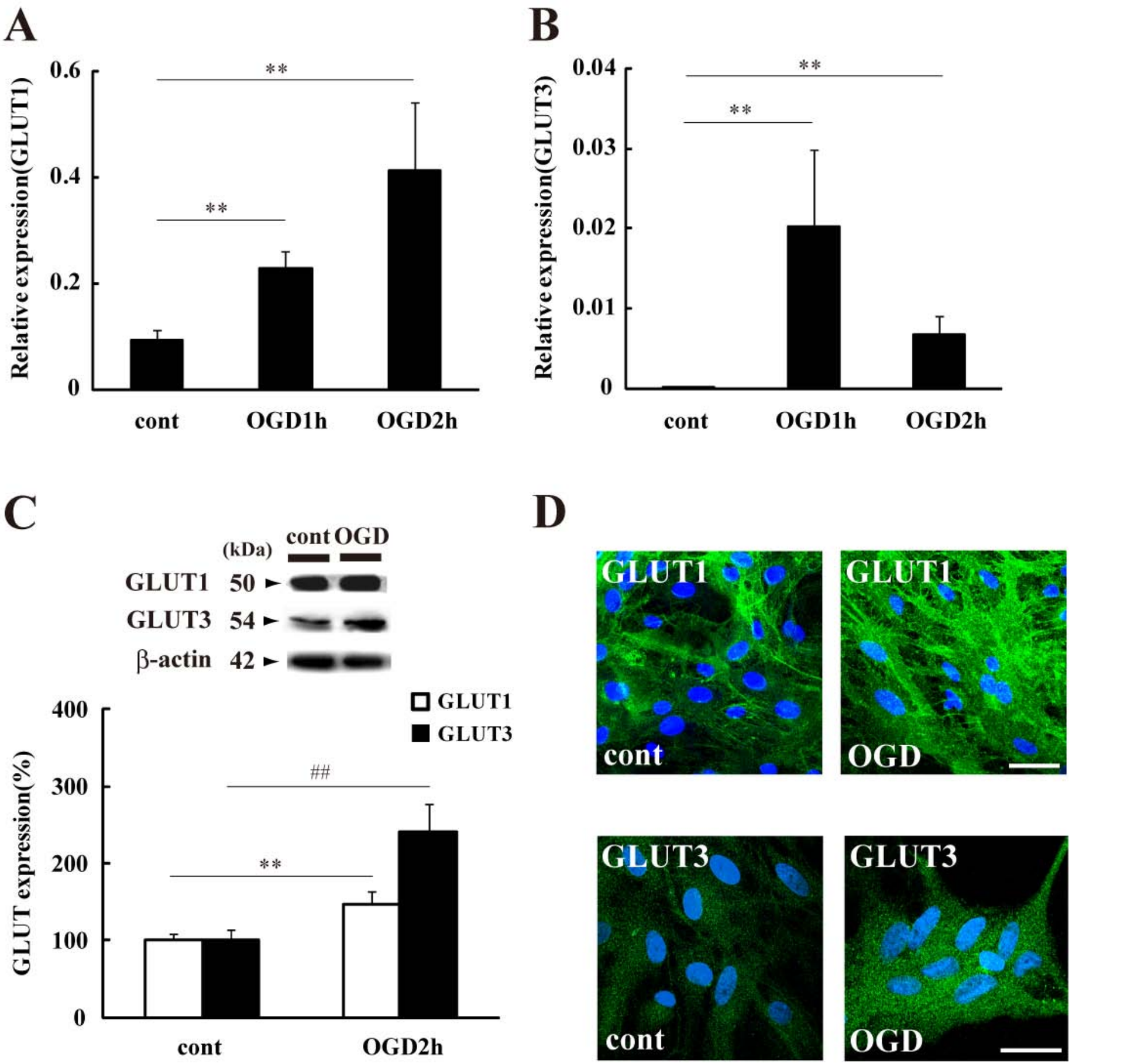
A
Relative expression(GLUT1)
0.6
0.4
0.2
0
**
**
cont
OGD1h
OGD2h
B
Relative expression(GLUT3)
0.04
0.03
0.02
0.01
0
**
**
cont
OGD1h
OGD2h
C
(kDa)
cont
OGD
GLUT1 50
GLUT3 54
β-actin 42
GLUT1
GLUT3
GLUT expression(%)
400
300
200
100
0
##
**
cont
OGD2h
D
GLUT1
cont
GLUT1
OGD
GLUT3
cont
GLUT3
OGD

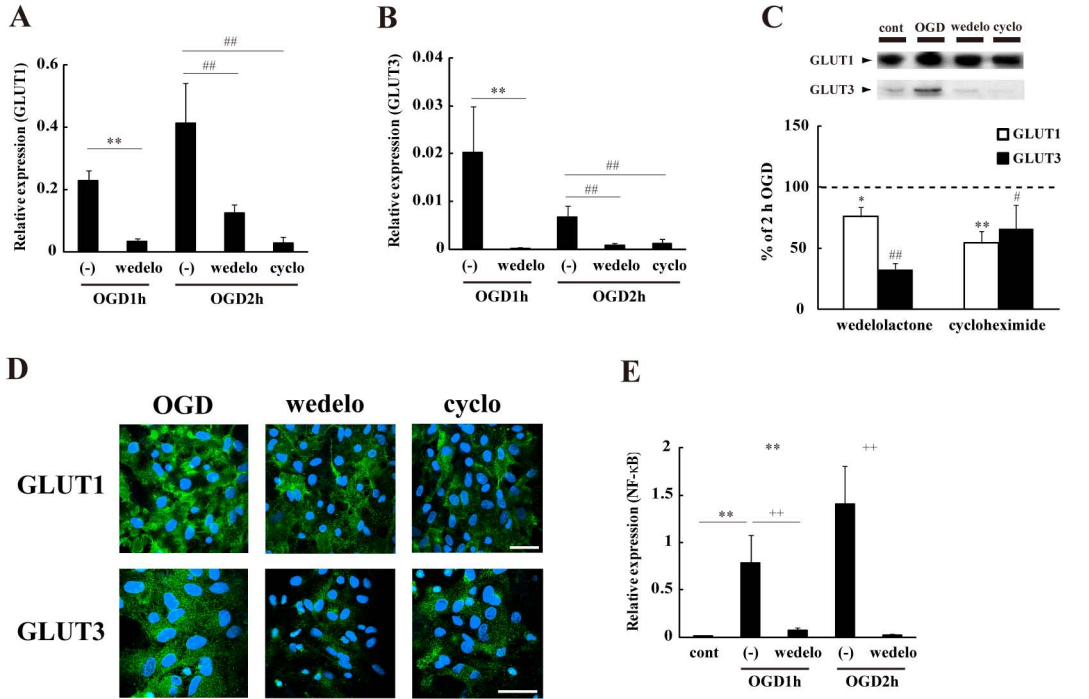
A
Relative expression (GLUT1)
0.6
0.4
0.2
0
**
##
##
(-)
wedelo
(-)
wedelo
cyclo
OGD1h
OGD2h
B
Relative expression (GLUT3)
0.04
0.03
0.02
0.01
0
**
##
##
(-)
wedelo
(-)
wedelo
cyclo
OGD1h
OGD2h
C
cont
OGD
wedelo
cyclo
GLUT1
GLUT3
150
100
50
0
% of 2 h OGD
GLUT1
GLUT3
*
##
**
#
wedelolactone
cycloheximide
D
OGD
wedelo
cyclo
GLUT1
GLUT3
E
Relative expression (NF-κB)
2
1.5
1
0.5
0
**
**
++
++
cont
(-)
wedelo
(-)
wedelo
OGD1h
OGD2h

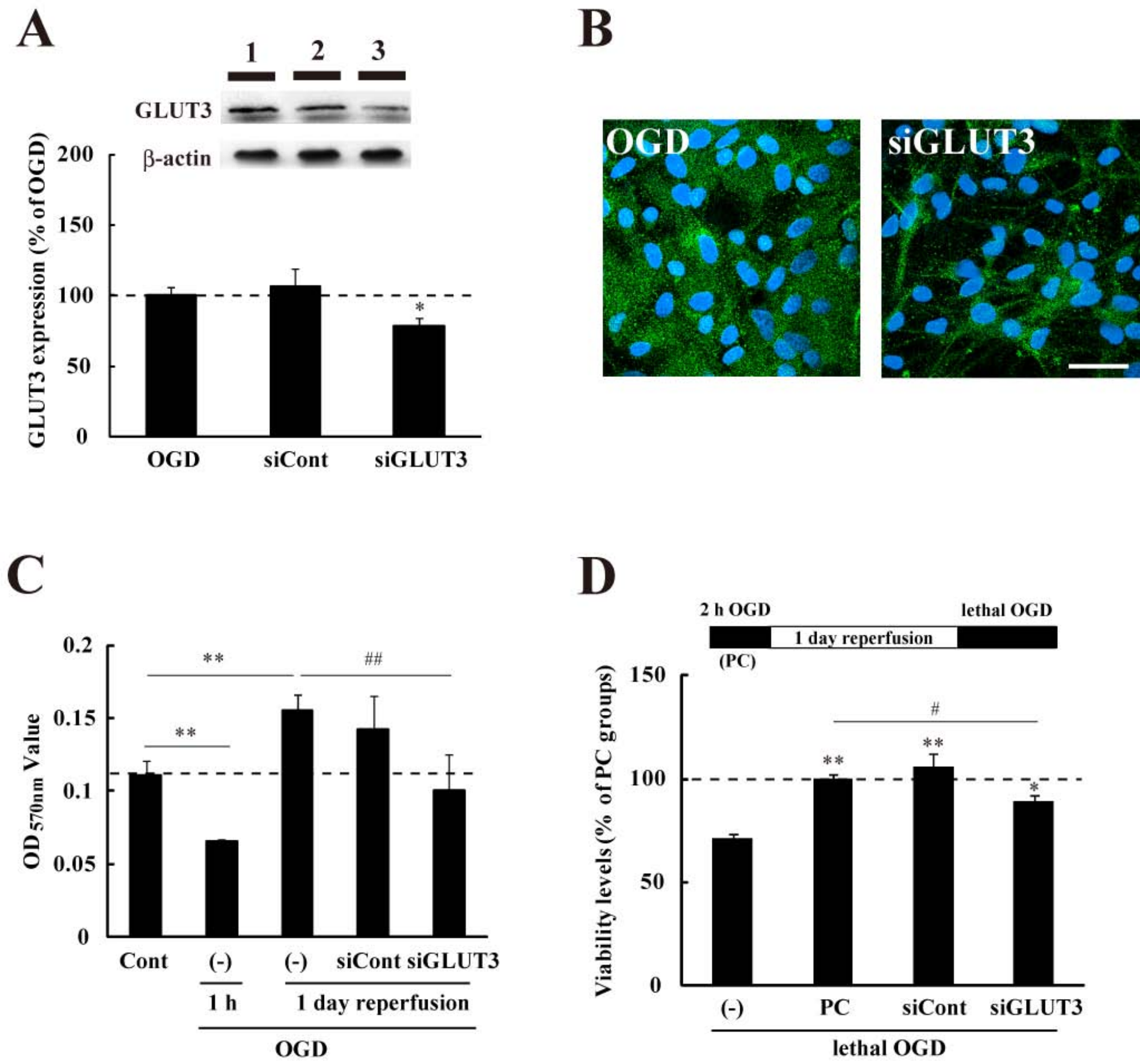
A
1
2
3
GLUT3
β-actin
GLUT3 expression (% of OGD)
200
150
100
50
0
*
OGD
siCont
siGLUT3
B
OGD
siGLUT3
C
0.2
0.15
0.1
0.05
0
OD570nm Value
**
**
##
Cont
(-)
(-)
siCont
siGLUT3
1 h
1 day reperfusion
OGD
D
2 h OGD
lethal OGD
1 day reperfusion
(PC)
Viability levels (% of PC groups)
150
100
50
0
#
**
**
*
(-)
PC
siCont
siGLUT3
lethal OGD

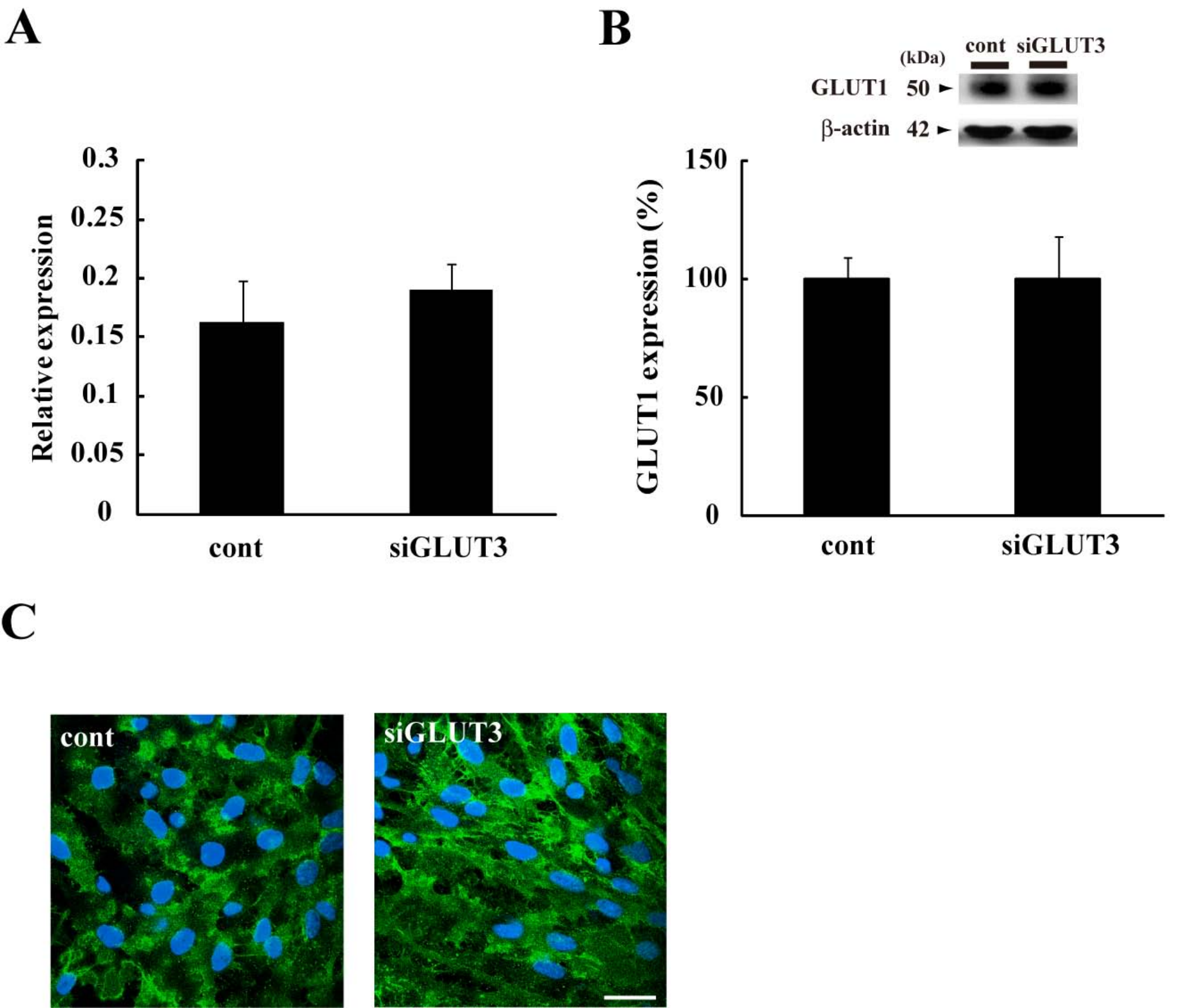
A
0.3
0.25
0.2
0.15
0.1
0.05
0
Relative expression
cont
siGLUT3
B
(kDa)
cont
siGLUT3
GLUT1
50
β-actin
42
150
100
50
0
GLUT1 expression (%)
cont
siGLUT3
C
cont
siGLUT3